SAND2011-7249C

12PFL-0127

Transmission Electron Microscopy of Soot Particles Directly Sampled in Diesel Spray Flame - A Comparison between US#2 and Biodiesel Soot

Tetsuya Aizawa, Hiroki Nishigai, Katsufumi Kondo and Teruo Yamaguchi
Meiji University
Jean-Guillaume Nerva
CMT, Universidad Politecnica de Valencia
Caroline Genzale
Georgia Institute of Technology
Sanghoon Kook
University of New South Wales
Lyle Pickett
Sandia National Laboratories

ABSTRACT

For a better understanding of soot formation and oxidation processes in conventional diesel and biodiesel spray flames, the morphology, microstructure and sizes of soot particles directly sampled in spray flames fuelled with US#2 diesel and soy-methyl ester were investigated using transmission electron microscopy (TEM). The soot samples were taken at 50mm from the injector nozzle, which corresponds to the peak soot location in the spray flames. The spray flames were generated in a constant-volume combustion chamber under a diesel-like high pressure and high temperature condition (6.7MPa, 1000K). Direct sampling permits a more direct assessment of soot as it is formed and oxidized in the flame, as opposed to exhaust PM measurements. Density of sampled soot particles, diameter of primary particles, gyration radius and fractal dimension of soot aggregates were analyzed and compared. No analysis of the soot micro-structure was made. The overall morphology of the biodiesel soot bears similarity to that of #2 diesel, but the soot density, primary particle size, and fractal dimension are smaller for biodiesel.

INTRODUCTION

For further and effective reduction of the particulate matter (PM) in the exhaust of a diesel engine, it is important to understand the properties and the microstructure of soot particles which reflect their formation and oxidation processes. There have been many studies on diesel soot morphology that include observations of soot particles sampled from the exhaust with electron microscopy [1-5]. However, in order to better understand the formation and oxidation processes of soot particles in the engine cylinder, it is necessary to investigate the morphology of soot particles inside a diesel spray flame. Recently, we have developed a technique to directly sample soot particles inside a diesel spray flame [6]. The benefits of this direct sampling compared to exhaust measurements include (1) analysis of soot particles formed in different regions in diesel spray flame, (2) back-to-back comparison with in-situ optical measurements, (3) avoidance of complicated condensation issues, dilution, SOF, or mixing with lube oil, in the exhaust, and (4) avoidance of possible continued aggregation as particles collide in the exhaust. In this work, we extend this soot particle sampling and analysis by Transmission Electron Microscopy (TEM) to include Soy-Methyl Ester biodiesel, aiming at a direct comparison of soot particle properties between the cases fuelled with the bio-diesel and conventional diesel. It has been reported that exhaust soot particles originating from bio-fuels exhibit oxidation rates and structure notably different from the ones from conventional diesel fuel [7-10]. This study aims to compare the morphology of soot particles directly sampled in the soy-methyl ester biodiesel and US#2

conventional diesel spray flames under an identical experimental condition. The greatest possible care was taken to acquire statistically reliable datasets of diameter of primary particles, gyration radius and fractal dimension of soot aggregates through a labor-intensive, manual processing of the TEM images of thousands of sampled soot particles.

EXPERIMENTAL SETUP

SOOT SAMPLING

Diesel combustion and soot sampling experiments were conducted using the optically-accessible constant volume combustion vessel at Combustion Research Facility of Sandia National Laboratories shown in Fig.1. Numerous studies on fundamental diesel spray combustion processes have been conducted using this facility via multiple optical diagnostic techniques. Ref. [11, 12] provide a detailed description of the vessel design, operating characteristics and experimental considerations. The vessel is cubic-shaped, 108mm on a side, and four sapphire windows are mounted on right, left, bottom, and front walls. A second-generation common-rail fuel injector with a single-hole nozzle is mounted on the top center and a fuel spray is injected into the center of the combustion vessel. More details on the injection hardware and rate of injection may be found in [11, 13]. A soot sampling probe is fixed on the opposed side wall to the injector. Fig. 2 shows example shadowgraphs of a diesel spray flame and the soot sampling probe taken in setup with uniform ambient temperature (up) and 2380μs after the start of fuel injection (bottom). A 3mm diameter carbon coated copper grid for TEM observation is mounted in the soot sampler. The probe is placed parallel to the spray axis to skim the gas containing soot from the spray flame while attempting to minimize flow disturbance at least to the upper half of the spray flame. The gas containing soot enters the probe through a 1mm diameter hole on a metal protection plate and soot particles are deposited on the cooler TEM grid via thermophoresis. Experimental conditions are summarized in Table 1. In the present study, low-sulfur US#2 diesel (US#2) and soy-methyl ester bio-diesel (BD) fuels were used as test fuels. The biodiesel fuel is a neat (100%) soy-derived biodiesel composed of five methyl esters; 11% methyl palmitate, 4% methyl stearate, 25% methyl oleate, 53% methyl linoleate and 7% methyl linolenate. More details of fuel properties have been reported elsewhere [14].

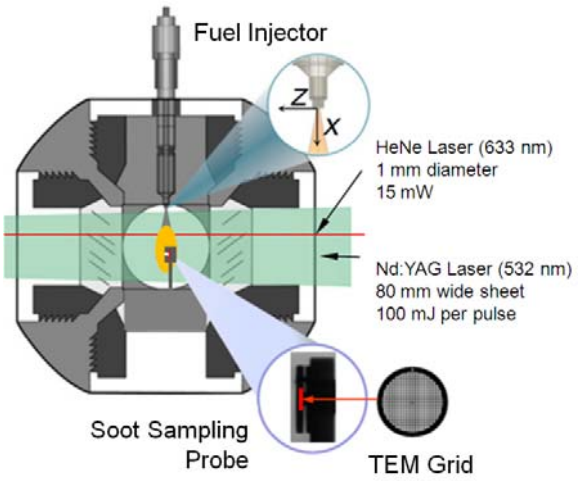

Figure 1 – Constant volume combustion vessel

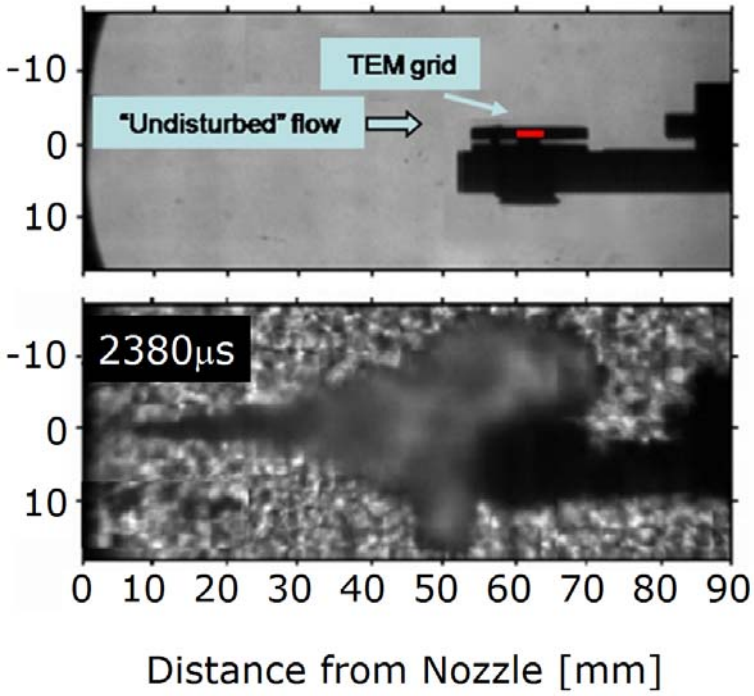

Figure 2 – Shadowgraphs of diesel spray flame and soot sampling probe

Table 1 – Experimental conditions

Surrounding conditions	
Gas density: ρ_a [kg/m^3]	22.8
Temperature: T_a [K]	1000
Pressure: P_a [MPa]	6.7
O_2 concentration: Xo_2 [%]	15
Injection conditions	
Nozzle	0.09mm×1
Injection pressure: P_{inj} [MPa]	150
Injection duration: Δt_{inj} [ms]	6
Fuel	US#2 low sulfur diesel (US#2) & Soy-Methyl Ester (BD)
Sampling conditions	
Distance from orifice: z [mm]	50
TEM grid type	carbon coated copper grid

In the present study, the soot sampled onto the TEM grid at 50mm from the nozzle for US#2 and bio-diesel cases were compared. The reason for the choice of the sampling location at 50mm from the nozzle is as follows. Figure.3 shows soot volume fraction measured in diesel spray flames fuelled with the US#2 and the BD fuels obtained by combining Planer Laser Induced Incandescence (PLII) and light extinction techniques. As shown in Fig.1, PLII was performed using a 80-mm-wide, 532-nm Nd:YAG laser sheet and simultaneously Light (Laser) Extinction was conducted using a helium-neon (HeNe) laser, which enabled the computation of the two-dimensional soot volume fraction. Details of the optical measurements are explained in references [6, 13]. Fig.3 shows that the soot volume fraction in the bio-diesel case is significantly lower than in the US#2 case. However, the relative profiles of soot distribution in the flame, showing a peak soot region around 50mm from the nozzle, are similar between the US#2 and BD cases. The flame lift-off locations, shown by dashed lines in Fig.3, are also similar between the two cases. Our previous observations on variation of soot morphology along different axial locations in spray flame have shown that the sizes of primary particles and aggregates of soot in spray flames exhibit the maximum around the peak soot region [15, 16]. Therefore, the comparison made in the present study is considered to be the one between the most grown-up soot directly sampled at the same location in the spray flames of different fuels under similar flame structure.

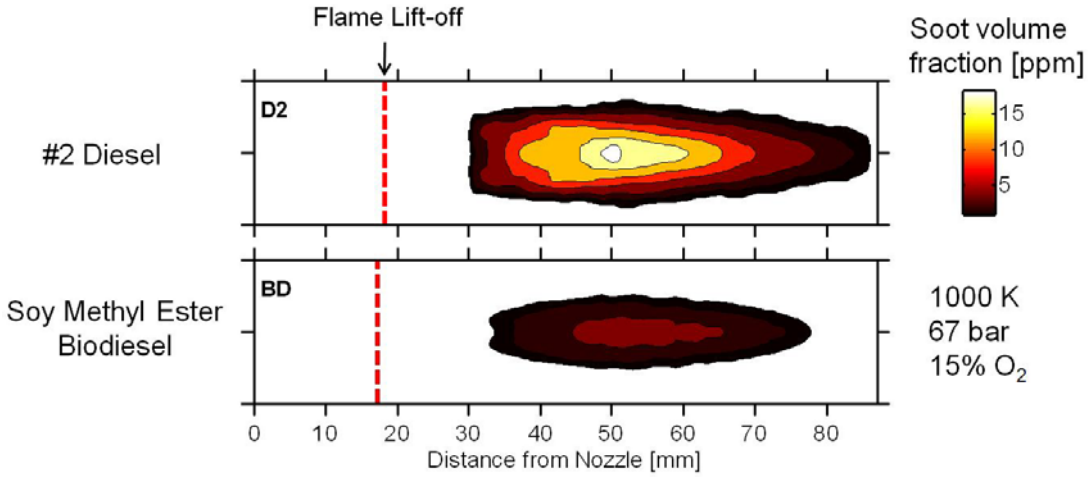

Figure 3 – Soot volume fraction distribution in quasi-steady diesel spray flames fuelled with US#2 and BD fuels

TEM OBSERVATION OF SAMPLED SOOT

Soot particles directly sampled in diesel spray flames onto the TEM grids fuelled with US#2 and BD fuels were observed by High-Resolution Transmission Electron Microscope, JEM-2100F (operating voltage: 200 keV, point resolution: 0.19nm) equipped with a CCD camera, Gatan Ultrascan 1000 / FIRST LIGHT (resolution: 2048×2048 pixels, physical pixel resolution: 14μm) at School of Science and Technology, Meiji University. The TEM grids were observed without any thermal or chemical pre-treatments to maintain properties of soot particles sampled in diesel spray flames as much as possible. One grid sample for each fuel was observed and more than 5 TEM images were taken at 5 different locations on each TEM grid as defined in Fig.4 with 2 different magnifications of x6,000 and x20,000, resulting in more than 100 TEM images to be analyzed. The time between sampling and the first TEM observation of the soot sample ranged from hours to months. Noticeable difference in the morphology, however, has not been observed in our general experience among samples with different storage duration up to years.

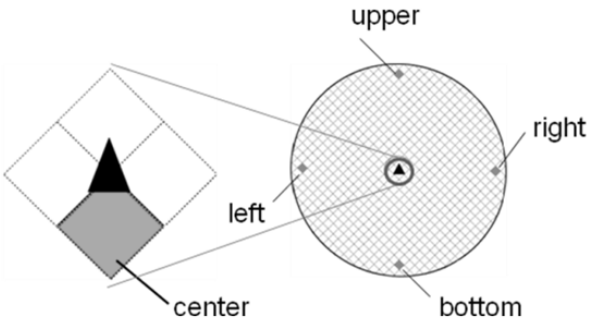

Figure 4 – Observation locations on TEM grids

TEM IMAGE ANALYSIS

Primary particle size, soot aggregate size and fractal dimension of soot particles are essential properties for characterizing and understanding the particulate growth process. The diameter of primary particle d_p, the radius of gyration of soot aggregate R_g and the projected area of soot aggregate A were acquired from TEM images using a software developed at the Combustion Research Facilities of Sandia National Laboratories and revised by the authors. The number of primary particles within an aggregate, n, was calculated by substituting the cross section of soot aggregates and primary particles $A_p = \pi d_p^2/4$ as shown in equation (1). The fractal dimension of soot particles was obtained following equation (2) [17] from the logarithmic plots of R_g/d_p and the n obtained from the equation (1). The radius of gyration of the soot aggregate, R_g, was calculated using the projected shape of each soot particle on binarized TEM images following the pixel-based equation (3). The mass of each soot aggregate was calculated using the mean primary particle size and the number of primary particles within each aggregate and the density of soot, which was assumed to be 2.0 g/cm^3 [18, 19].

$$n = \left(\frac{A}{A_p} \right)^{\alpha} \qquad (1)$$

$$n = k_f \left(\frac{R_g}{d_p} \right)^{D_f} \qquad (2)$$

$$R_g^2 = \frac{1}{m} \sum r_i^2 \qquad (3)$$

n : number of primary particles per aggregate
A : projected area of soot aggregate [nm^2]
A_p : primary particle cross section [nm^2]
α : exponential factor for particle overlap (=1.09) [20]
k_f : pre-factor
D_f : fractal dimension of soot particle
R_g : radius of gyration of soot aggregate [nm]
d_p : averaged diameter of primary particle [nm]
m : number of pixels per aggregate
r_i : distance between each pixel and centroid of soot aggregate [nm]

RESULTS

TEM IMAGES OF SOOT AND PROJECTED AREA RATIO

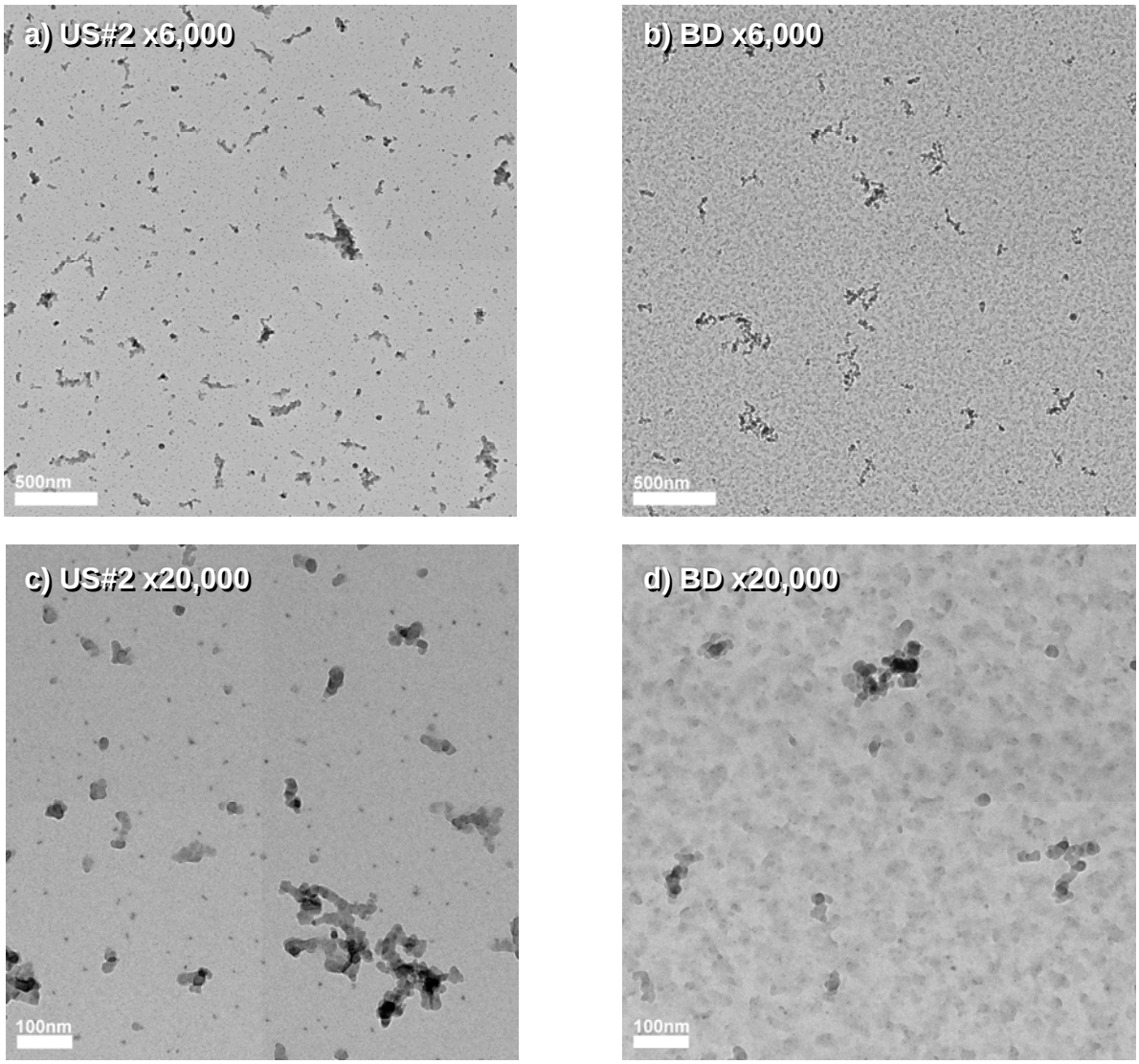

Figure 5 –Sample TEM images of soot particles directly sampled in diesel spray flame fuelled with US#2 and bio-diesel fuels at 50mm from the injector nozzle

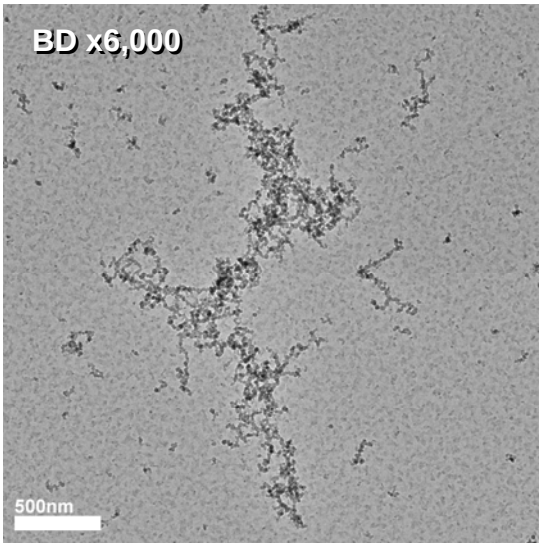

Figure 6 – TEM image of exceptionally large soot aggregate sampled in bio-diesel spray flame

Fig.5 shows example TEM images of soot particles directly sampled in diesel spray flame fuelled with US#2 and BD fuels. Fig.5 (a) to (b) and (c) to (d) compare TEM images of soot particles of US#2 and BD fuels at x6000 and x20000 different magnifications, respectively. The amount of soot particles sampled onto the grid is clearly smaller for the BD case, which is consistent with the optical soot measurements in the spray flame shown in Fig.3. Note that single primary particles and soot aggregates coexist in all images, suggesting that the aggregation process is in progress at this peak-soot sampling location, 50mm from the nozzle. One may notice that the TEM images for BD case exhibit "busy" background with faint spot-like features compared to the US#2 case. This busy background was observed more frequently, but not exclusively, for BD case images. The spot-like features are smaller and planar than soot particles were not considered in the analysis. Experience showed that they also did not interfere with primary particle or soot aggregate metrology from which the statistics of this paper are derived.

Fig.6 shows a TEM image example of significantly larger soot aggregates of over 1μm size at x6000 magnification, which were observed only for the BD fuel case. Typical soot aggregates observed in diesel exhaust is known to be up to few hundred nm as frequently reported in literatures [2, 7, 9, 10]. The fact that these significantly larger aggregates were observed only for the BD case, in which the optically measured soot volume fraction and the amount of soot observed on the TEM grid are clearly smaller than for the US#2 case, implies that the aggregation mechanism of soot in the spray flame may be different between these fuels.

Fig. 7 shows projected area ratio of soot particles sampled onto the grid surface calculated by binarizing the TEM images. Note that this projected area ratio is the average among the 5 different locations on the grid shown in Fig.4, in which the center had about twice the soot of the other 4 locations because it is directly facing the 1mm diameter hole on the plate covering the grid. The projected area ratio of BD fuel case is about half lower than for the US#2 case, which is consistent with the general trend of the optically measured soot volume fraction shown in Fig.3. Therefore, the amount of soot sampled onto the TEM grid in the spray flame is considered to reasonably reflect the soot concentration in the spray flame.

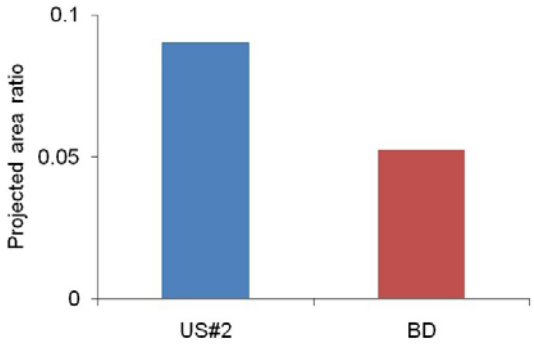

Figure 7 – Projected area ratio of soot particles on TEM grids

DIAMETER OF PRIMARY PARTICLES

The primary diameter measurements were based on TEM images at a magnification of x20,000, which is useful for identification of each primary particle within aggregates and at the same time the number of particle samples in the view field is statistically acceptable. As shown in Fig.8, which is a GUI screenshot of the MATLAB-based image analysis software, the primary diameter measurement is not a simple "image analysis" process, but it is based on the recognition, by the operator, of a complicated 3D shape and structure of soot aggregate only from its projected TEM image. In the present research, only apparently identifiable primary particles, including the separately existing single primaries and the ones within the aggregates, were measured. It has been confirmed that the distribution and the mean of primary diameter is not biased by this selective sampling of apparently identifiable primary particles [15, 21]. The diameter measurements were conducted at biaxial directions for each primary particle, because many primary particles exhibited non-round shapes. The entire diameter measurement in the present research was completed by an experienced single operator in order to avoid any operator dependency on the measurement results between the different fuel cases. Our ongoing examination show that the operator dependency on the resulting mean diameter could be up to few nm, especially among less experienced operators.

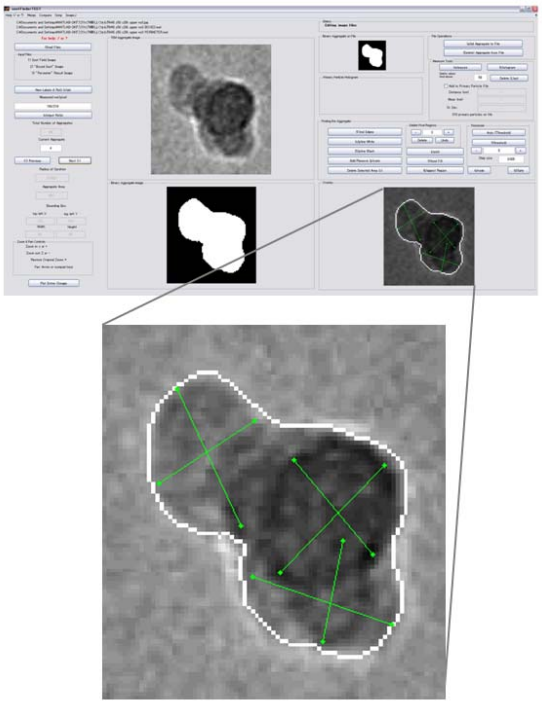

Figure 8 – GUI screenshot of MATLAB-based image analysis software

Fig.9 compares normalized histograms of primary particle diameter for soot directly sampled in diesel spray flames fuelled with US#2 and BD fuels. The numbers of measurements of primary particles for US#2 and BD fuel cases were 4720 and 5336, respectively. The diameter of many primary particles ranged from 10nm to 30nm and the size histogram spread like a normal distribution. The histogram profiles resemble each other between US#2 and BD cases, but the histogram of BD case seems to be slightly shifted to left. The arithmetic mean diameters for US#2 and BD fuel cases were 18.4 and 16.9 nm, respectively, which corresponds to about 9% smaller diameter for BD case. A commonly applied statistical t-test assuming normal distribution with unequal sample size and variance shows that the difference between the two means is significant with 95% confidence.

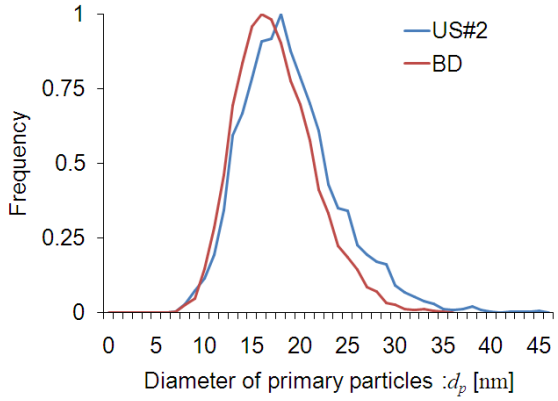

Figure 9 – Normalized histogram of primary particle diameter for US#2 and BD cases

GYRATION RADIUS OF SOOT AGGREGATES

Fig.10 shows the mass-based distribution of gyration radius of soot aggregates directly sampled in diesel spray flames fuelled with US#2 and BD fuels. The gyration radius was obtained using the projected shape of each aggregate on binarized TEM images at a magnification of x6,000. The x6,000 magnification images are suitable for observation of projected shape of each soot aggregate and at the same time they produce a large number of samples for statistically reliable analysis. Note that in this analysis the soot "aggregates" include not only aggregates, but also separately existing single primary particles and small aggregates consisting of only several primary particles. It should also be noted that the primary particle size is in "diameter", while the aggregate size is in "radius". The number of analyzed soot aggregates was 2325 and 1517 for US#2 and BD fuel cases, respectively. The size distribution did not exhibit any noticeable difference among the 5 different locations on the grid shown in Fig.4. Fig.10 shows that the mass of soot aggregates are clearly smaller for the BD case, which is consistent with the optically measured soot concentration shown in Fig.3. However, the mass-weighted mean gyration radius for BD fuel case was 64.8nm, which was larger than the US#2 case of 44.3nm. Fig.10 shows that relatively larger soot aggregates over 150nm of gyration radius are observed only for the BD fuel case. As mentioned above, significantly larger soot aggregates of over 1μm size, which have been omitted from the statistics and the histogram shown in Fig.10, were also observed only for the BD fuel case. The fact that the larger aggregates are observed in a less sooting BD spray flame may imply that the aggregation mechanism of soot in spray flame differs between US#2 and BD fuel cases.

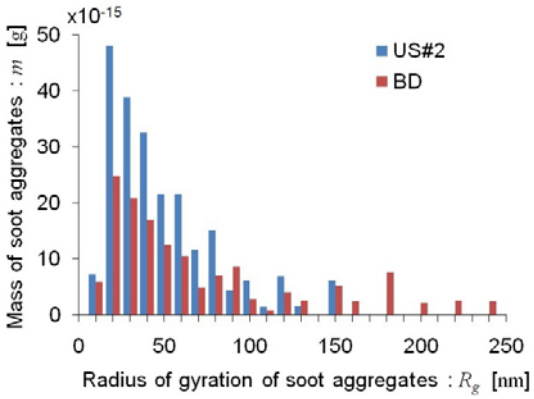

Figure 10 – Mass-based histogram of gyration radius of soot aggregates for US#2 and BD cases

FRACTAL DIMENSION

Fractal dimension of soot particles, which is an indicator of structural characteristics of soot aggregates, were analyzed. The calculation of fractal dimension requires the mean diameter of primary particles in each soot aggregate. Therefore, the TEM images at x20,000 magnification, which are useful for observation and identification of primary particles within the aggregate, were used for the analysis of the fractal dimension. Fig.11 shows logarithmic plots of n vs. R_g/d_p for the calculation of fractal dimension of soot particles directly sampled in diesel spray flames with US#2 and BD fuels. Although Fig.11 includes all plots representing not only aggregates but also down to single primary particles, the fractal dimension was calculated excluding aggregates with n of less than 3, i.e. monomer and dimer, because they are neither aggregate nor fractal. The distribution did not exhibit any noticeable systematic differences among the 5 different locations on the grid shown in Fig.4. The slope of the linear regression line represents the fractal dimension D_f. The obtained fractal dimensions for the BD case of 1.66 was smaller than the one for the US#2 case of 1.76, which means that soot aggregates originating from BD fuel are less compacted than the ones from US#2 fuel.

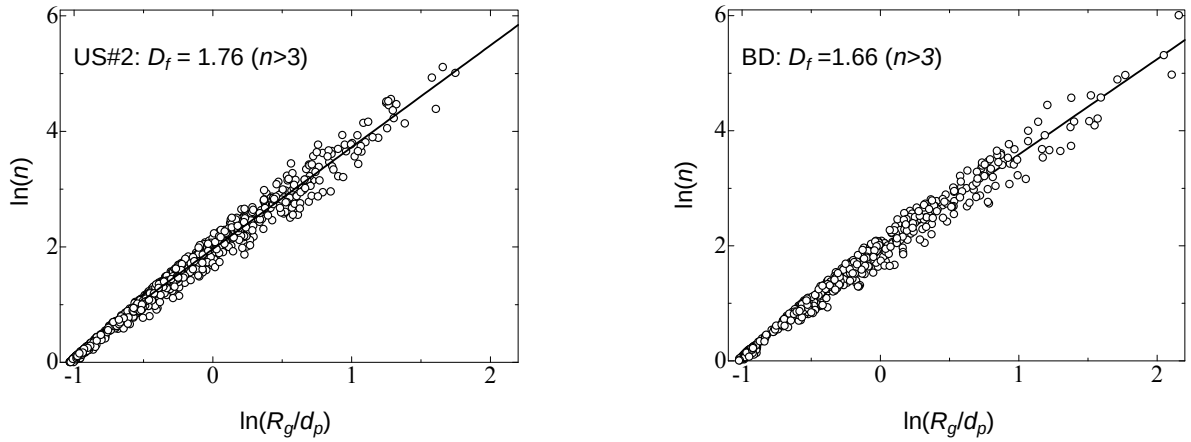

Figure 11 –Logarithmic plots of R_g/d_p for soot in US#2 and bio-diesel spray frames. Each open circle represents measured soot aggregates. The slope of the linear regression line represents the fractal dimension D_f

CONCLUSIONS

Soot particles were directly sampled in diesel spray flames fuelled with conventional diesel (US#2) and soy-methyl ester bio-diesel (BD) fuels at a peak soot location of 50mm from the nozzle. The soot samples were observed by transmission electron microscopy (TEM) and projected area ratio, primary particle diameter, gyration radius and fractal dimension of the sampled soot particles were analyzed and compared between the two fuel cases. The conclusions obtained in this study are as follows:

1) Projected area ratio, total number and mass of soot particles sampled onto the TEM grid surface in the spray flames were smaller for BD fuel case than for US#2, the trend of which was consistent with optically measured soot volume fraction in these spray flames.

2) The arithmetic means of primary particle diameter for US#2 and BD fuel cases were 18.4 and 16.9 nm, respectively, which corresponds to about 9% smaller diameter for BD case.

3) Although the optically measured soot concentration in the flame, the number and the mass of sampled soot aggregates were smaller for BD fuel case than for US#2, the mass-weighted mean gyration radius for BD fuel case (64.8nm) was larger than the one for US#2 case (44.3nm). Relatively larger soot aggregates over 150nm of gyration radius were observed only for the BD fuel case.

4) The fractal dimensions for BD case of 1.66 was smaller than the one for US#2 case of 1.76, indicating that soot aggregates originating from BD fuel are less compacted than the ones from US#2 fuel.

ACKNOWLEDGMENTS

Support for this research was provided by the U.S. Department of Energy. A part of this research was performed at the Combustion Research Facility, Sandia National Laboratories, Livermore, California. Sandia is a multi-program laboratory operated by Sandia Corporation, a Lockheed Martin Company, for the United States Department of Energy's National Nuclear Security.

The authors would also like to acknowledge the Spanish Ministry of Science and Innovation for supporting Jean-Guillaume Nerva's visiting research at both SNL and Meiji University, through the OPTICOMB project (TRA2007-67961-C03-01).

Authors are sincerely grateful to Hideyuki Yoshimura of Department of Physics, Meiji University for providing with the opportunity to use the HRTEM for soot observation, and to Yoshimitsu Nagai of Department of Mechanical Engineering Informatics, Meiji University for his valuable advices on statistical analysis.

REFERENCES

1. T. Ishiguro, Y. Takatori and K. Akihama: Microstructure of Diesel Soot Particles Probed by Electron Microscopy: First Observation of Inner Core and Outer Shell, *Combust. Flame*, Vol.108, pp.231-234 (1997).
2. K.O. Lee, R. Cole, R. Sekar, M. Y Choi, J.S. Kang, C.S. Bae and H.D. Shin, Morphological Investigation of the Microstructure, Dimensions, and Fractal Geometry of Diesel Particulates, Proceedings of Combustion Institute, Vol. 29, pp.647-653 (2002).
3. K. Tian, K.A. Thomson, F. Liu, D.R. Snelling, G.J. Smallwood and D. Wang, Determination of the Morphology of Soot Aggregates Using the Relative Optical Density Method for the Analysis of TEM images, Combustion and Flame, Vol. 144, pp. 782-791 (2006).
4. B.F. Kock, B. Tribalet, C. Schulz and P. Roth, Two-color time-resolved LII applied to soot particle sizing in the cylinder of a Diesel engine, Combustion and Flame, Vol. 147, pp. 79-92 (2006).
5. M. Lapuerta, F.J. Martos and J.M. Herreros, Effect of engine operating conditions on the size of primary particles composing diesel soot agglomerates, Journal of Aerosol Science, Vol. 38, pp. 455-466 (2007).
6. S. Kook and L.M. Pickett, Soot Volume Fraction and Morphology of Conventional and Surrogate Jet Fuel Sprays at 1000-K and 6.7-MPa Ambient Conditions, Proc. Combust. Inst., Vol. 33, pp 2911–2918 (2011).
7. A.L. Boehman J. Song and M. Alam, Impact of Biodiesel Blending on Diesel Soot and the Regeneration of Particulate Filters, Energy & Fuels, Vol.19, pp. 1857-1864 (2005).
8. R.L. Vander Wal and C.J. Mueller, Initial Investigation of Effects of Fuel Oxygenation on Nanostructure of Soot from a Direct-Injection Engine, Energy & Fuels, Vol.20, pp. 2364-2369 (2006).
9. K. Yehliu, A.L. Boehman and O. Armas, Emission from Different Alternative Diesel Fuels Operating with Single and Split Fuel Injection, Fuel, Vol.89-2, pp. 423-437 (2010).
10. O. Armas, K. Yehliu and A.L. Boehman, Effect of Alternative Fuels on Exhaust Emissions during Diesel Engine Operation with Matched Combustion Phasing, Fuel, Vol. 89-2, pp. 438-456 (2010).
11. Engine Combustion Network experimental data archive, http://www.ca.sandia.gov/ECN/.
12. L.M. Pickett, C.L. Genzale, G. Bruneaux, L.-M. Malbec, L. Hermant, C. Christiansen and J. Schramm, Comparison of diesel spray combustion in different high-temperature, high-pressure facilities, SAE Paper 2010-01-2106 (2010).
13. J.-G. Nerva, C.L. Genzale, S. Kook, J.M. García-Oliver and L.M. Pickett, Fundamental Spray and Combustion Measurements of Biodiesel under Diesel Steady Conditions, manuscript in preparation.
14. C.L. Genzale and L.M. Pickett, Liquid Penetration of Diesel and Biodiesel Sprays at Late-Cycle Post-Injection Conditions, SAE Paper 2010-01-0610 (2010).
15. J.-G.Nerva, T.Yamaguchi, H.Iguma, H.Nishigai, K.Kondo, S.Takano, T.Aizawa, C.L.Genzale, L.M.Pickett, Transmission Electron Microscopy of Soot Particles Sampled Directly from a Biodiesel Spray Flame, Proc. 2011 JSAE/SAE International Powertrains, Fuels & Lubricants Meeting, Paper No. JSAE 20119164 / SAE 2011-01-2046 (2011).
16. K.Kondo, T.Yamaguchi, H.Nishigai, S.Takano, T.Aizawa, High-Resolution Transmission Electron Microscopy of Soot Directly Sampled at Different Axial Locations in Diesel Spray Flame, Proc.10th International Conference on Engines & Vehicles, Paper No. SAE 2011-24-0068 (2011).
17. K. O. Lee, C. M. Megaridis, S. Zelepouga, A. V. Saveliev and L. A. Kennedy, Soot Formation Effects of Oxygen Concentration in the Oxidizer Stream of Laminar Coannular Nonpremixed Methane/Air Flames, *Combust. Flame*, vol.121, pp.323-333 (2000).
18. J. B. Heywood, *Internal Combustion Engine Fundamentals*, p.631, 645 and 646, McGraw-Hill (1988).
19. H. Bockhorn (ed.), *Soot Formation in Combustion – Mechanisms and Models*, p.177 and 427, Springer-Verlag (1994).
20. C. M. Megaridis and R. A. Dobbins, Morphological Description of Flame- Generated Materials, *Combust. Sci. Technol.*, vol.71, pp.95-109 (1990).

21. T.Yamaguchi, K.Kondo, H.Nishigai, S.Takano, T.Aizawa, Direct Sampling, TEM Analysis and Optical Measurement of Soot Particles at Different Axial Locations in a Transient Spray Flame, Proc. 2011 JSAE/SAE International Powertrains, Fuels & Lubricants Meeting, Paper No. JSAE 20119152 / SAE 2011-01-2051 (2011).